EMULSIONS STABILISED BY WHEY PROTEIN MICROGEL PARTICLES: TOWARDS FOOD-GRADE PICKERING EMULSIONS

Mathieu Destribats,[a,†] Martine Rouvet,[b] Cécile Gehin-Delval,[b] Christophe Schmitt[b] and

Bernard P. Binks[a,*]

[a] *Surfactant & Colloid Group, Department of Chemistry, University of Hull, Hull. HU6 7RX. UK*

[b] *Department of Food Science and Technology, Nestlé Research Center, Vers-chez-les-Blanc, P.O. Box 44, CH-1000 Lausanne 26, Switzerland*

[†] *Currently at L'ORÉAL, 11 rue Dora Maar, 93400 Saint-Ouen, France*

*Proofs and correspondence to: Professor B.P. Binks
b.p.binks@hull.ac.uk

ABSTRACT

We have investigated a new class of food-grade particles, whey protein microgels, as stabilisers of triglyceride-water emulsions. The sub-micron particles stabilized oil-in-water emulsions at all pH with and without salt. All emulsions creamed but exhibited exceptional resistance to coalescence. Clear correlations exist between the properties of the microgels in aqueous dispersion and the resulting emulsion characteristics. For conditions in which the particles were uncharged, fluid emulsions with relatively large drops were stabilised, whereas emulsions stabilized by charged particles contained smaller flocculated drops. A combination of optical microscopy of the drops and spectrophotometry of the resolved aqueous phase allowed us to estimate the interfacial adsorption densities of the particles using the phenomenon of limited coalescence. We deduce two classes of particle arrangement. Complete adsorption of the particles was obtained when they were neutral or when their charges were screened by salt resulting in at least one particle monolayer at the interface. By contrast, only around 50% of the particles adsorbed when they were charged with emulsion drops being covered by less than half a monolayer. These findings were supported by direct visualization of drop interfaces using cryo-scanning electron microscopy. Uncharged particles were highly aggregated and formed a continuous 2-D network at the interface. Otherwise particles organized as individual aggregates separated by particle-free regions. In this case, we suggest that some particles spread at the interface leading to the formation of a continuous protein membrane. Charged particles displayed the ability to bridge opposing interfaces of neighbouring drops to form dense particle disks protecting drops against coalescence; this is the main reason for the flocculation and stability of emulsions containing sparsely covered drops.

Keywords: Pickering emulsions, microgel, whey protein, limited coalescence

INTRODUCTION

Emulsions are dispersions of immiscible liquids as, for example, oil drops dispersed in water (o/w or direct emulsions) or water drops dispersed in oil (w/o or reverse emulsions). Due to their inherent metastable state, these systems irremediably tend towards macroscopic phase separation which corresponds to their lower energy state. In order to kinetically stabilize emulsions and slow down their destruction, low molecular weight surface-active agents (surfactants) or macromolecules (such as proteins or polymers) are most commonly used as emulsifier, both decreasing the interfacial tension and ensuring steric and/or electrostatic repulsions between drop interfaces. However, since the pioneering work of Ramsden and Pickering[1,2] more than a century ago, colloidal particles are also known to be efficient interface stabilizers and the obtained emulsions are nowadays referred to as particle-stabilized emulsions or Pickering emulsions in the literature [3,4].

For adsorption at an interface, particles are required to be partially wetted by both phases. According to the empirical rules[5,6], the emulsion type (o/w or w/o) is mainly determined by the relative particle wettability in both liquids, the most wetting liquid becoming the continuous phase. This relative particle wettability for spherical particles is expressed in terms of the contact angle θ which is the angle between the interface and the tangent to the particle-water interface at the point where the three phases meet. In mixtures of equal volumes of the two immiscible fluids, for preferentially hydrophilic (respectively hydrophobic) particles, the contact angle is smaller (larger) than 90° and o/w (w/o) emulsions are preferentially obtained. In the case of a spherical particle small enough (less than few microns in diameter) to neglect the effect of gravity, the free energy E required to remove it from the interface can be estimated through the following equation:

$$E = \gamma \pi a^2 (1 - |\cos\theta|)^2 \tag{1}$$

where γ is the bare oil-water interfacial tension and a is the particle radius. It appears then that even for nanometre-sized particles, the desorption energy can easily reach several thousands of $k_B T$ (where k_B is the Boltzmann constant and T is the absolute temperature) and that the particle anchorage at the interface may be considered as irreversible provided that θ is not close to the limiting values (0 or 180°) .[3] This characteristic associated with the ability of particles to develop strong interactions at interfaces to form rigid layers protecting the drops is the origin of the outstanding stability of Pickering emulsions towards coalescence and disproportionation. Due to these peculiar properties, this field has been an active research area during the last decade and numerous novel materials have been proposed such as biliquid foams[7,8], highly stable double emulsions[7,9], liquid marbles[10,11], powdered emulsions and dry water[12-14] or highly stable foams[15,16] to name but a few.

Very often food systems contain in their formulation colloidal particles and it is well established that some of them participate in the stabilization of emulsions or foams by adsorbing at the interface, as is the case for fatty acid crystals in margarines or spreads or aggregated crystallized emulsion drops in whipped cream products.[17,18] Food structuring science appears then like a natural field of application where the original properties of interface stabilization by particles could be advantageously used to design food formulations with novel textures, enhanced encapsulation efficiencies or better stability and quality. However, much of the fundamental work realized so far on Pickering emulsions involved organic or inorganic model particles, such as silica or latex particles, which are not approved as food-grade materials. One of the ongoing challenges is then to identify or produce cheap and food compliant colloidal particles acting as effective stabilizers that could be used on a commercial scale. Up to now, a limited but recently growing number of interesting food-grade particles for emulsion stabilization have been proposed amongst which are cellulose microparticles or nanocrystals[19,20], chitin nanocrystals[21], soy protein particles[22,23], modified starch particles[24-26], flavonoid particles[27], solid lipid nanoparticles[28] or zein protein particles[29].

In that context, we report herein the study of another class of protein-based particles as emulsion stabilizer. It is well established that globular whey proteins under specific processing conditions (of temperature, pressure, salinity and pH) can self assemble into different kinds of aggregates[30]. The whey protein aggregates used in this study were covalently cross-linked and named hereafter whey protein microgel (WPM) particles. Commercial whey protein isolate was used as the starting material and the synthesis pathway allowed a large scale production of particles by a combination of fast heat treatment in a plate-plate exchanger, microfiltration and spray drying resulting in powdered WPM as described in a previous publication.[31] In the present paper we characterize the behavior of the re-dispersed WPM particles in aqueous dispersions or at the oil-water interface of o/w emulsions as a function of the pH and salinity of the aqueous phase. We use macroscopic visualization and optical microscopy to characterize the emulsion properties. In particle-stabilised emulsions, if the total amount of particles is initially insufficient to cover the drop interfaces, the drops coalesce such that the total interfacial area between oil and water is progressively reduced. Since it is likely that the particles are irreversibly adsorbed, the degree of surface coverage by them increases until coalescence is halted, a process known as limited coalescence.[8] By coupling a study of the limited coalescence phenomenon occurring in Pickering emulsions with spectrophotometry measurements and cryo-scanning electron microscopy (SEM) observation of the emulsion interfaces, we determine the adsorption density of the particles and their organization and show that they adsorb differently depending on the pH and salinity, either forming a dense 2-D network of aggregated particles or by leaving the drops poorly protected with sparsely distributed particle aggregates. In this latter case, we evidence bridging events between drops as the origin

of the flocculation of the emulsions. All emulsions exhibited exceptional long-term resistance to coalescence when their surface coverage by WPM particles was high, as demonstrated by the formation of emulsions with millimeter drop sizes.

EXPERIMENTAL

Materials

Water was purified by passing through an Elgastat Prima reverse osmosis unit followed by a Millipore Milli-Q reagent water system. The food-grade oil Miglyol 812N (mixture of caprylic C_8 and capric C_{10} triglycerides, Sasol, density at 20 ºC = 0.945 g/cm^3), heptane (Sigma-Aldrich, > 99%) and sodium azide (Sigma, > 99%) were used as received. For preservative purposes, all the prepared aqueous phases contained 0.01 wt.% of NaN_3. Covalently cross-linked whey protein microgel particles (WPM) were received as a spray-dried powder from Nestlé Research Center, Lausanne. The preparation of the microgels is the result of a complex interplay of heat denaturation of the whey proteins, aggregation, electrostatic repulsion and formation of inter- or intra-protein disulfide bonds. Details of large scale WPM synthesis have been already reported in a recent publication[31] but can be summarized here. The WPM particles were obtained by heat treatment of a dispersion of whey protein isolate, WPI (Prolacta 90, Lactalis, France), at 4 wt.% protein in softened water (160 mg/L Na^+) at pH 5.9. The WPI dispersion was pre-heated to 60 °C and then heated to 85 °C using a Soja plate-plate heat-exchanger (PHE) operating at a flow rate of 1000 L/h, followed by a holding time of 15 min. in a tubular heat exchanger and subsequent cooling to 4 °C. This treatment promoted the conversion of 85% of the initial proteins into disulfide bond cross-linked microgel particles characterized by a mean diameter of ~280 nm and a low polydispersity index (< 0.1). Then the dispersion was concentrated to 22 wt.% by microfiltration before been spray-dried using a GEA Niro SD6.3N spray dryer (Søborg, Denmark).

Methods

(a) *Preparation of WPM particle dispersions*

For the preparation of the WPM dispersions, the WPM powder was dispersed at 4 wt.% in 10 mL water for 30 min. under mild magnetic stirring prior to sonication with an ultrasound probe (Branson Digital Sonifier, probe head diameter 6 mm, 30% amplitude, 1 s pulse on, 0.5 s pulse off) for 20 min. During sonication, the dispersion was immersed in an ice bath to avoid excessive heating of the sample (temperature measured at the end < 45 °C).

(b) *Size and ζ-potential measurements of WPM dispersions*

The hydrodynamic diameter of the WPM particles was measured by dynamic light scattering at 25 °C using a Nanosizer ZS instrument (Malvern Instruments) set in backscattering configuration. Samples were diluted to 0.01 wt.% before measurement and placed in disposable square polystyrene cuvettes (DTS0012). The hydrodynamic diameter and the polydispersity index were calculated by the cumulant analysis method of the autocorrelation function. The zeta ζ-potential of 0.01 wt.% WPM dispersions was determined between pH 2 and 8 at 25 °C by light scattering upon application of an alternating electrical field by the probe used in its dip cell configuration. The effective electrical field applied in the measurement cell varied between 3 and 40 V depending on the ionic strength of the dispersions. The electrophoretic mobility was calculated assuming spherical particles and the ζ-potential was then deduced using the Schmoluchoski equation.[32]

Transmission electron microscopy (TEM) was also employed for particle dispersions. The samples were prepared using the negative-staining method as follows. A drop of the WPM dispersion was deposited onto a carbon support film mounted on a copper grid. The excess product was removed after 30 sec. using filter paper. A droplet of 1% phosphotungstic acid at pH 7 was added over 15 sec., any excess being removed as before. The samples were observed using a Philips CM12 transmission electron microscope operating at 80 kV. Images were recorded by a Gatan Multiscan camera (model 794).

(c) *Measurement of oil-water interfacial tension*

The oil-water interfacial tensions of aqueous particle dispersions in contact with Miglyol 812N were measured using the du Noüy ring method (Krüss K10 digital tensiometer). The platinum ring was hung on a hook at the bottom of an electronic balance of 0.1 mg sensitivity. The measuring vessel was placed in a glass jacket on a perpendicularly moveable platform. The jacket was circulated by water at 25 °C from a thermostat. The ring was immersed in the aqueous solution by raising the platform and the oil phase was carefully added. The ring was then pulled out by lowering the platform slowly creating a meniscus at the oil-water interface and the interfacial tension was then recorded using the maximum-pull method. Each measurement was reproduced at least 3 times to obtain an average. The value of the interfacial tension was then corrected by multiplying the measured maximum force F (in mN/m) by the appropriate correction factor.[33]

(d) *Emulsion preparation and characterization*

Typical emulsions were composed of identical volumes of water and oil phases (50/50 vol.%) for a total volume of 10 mL with various concentrations of WPM initially dispersed in the aqueous phase. The aqueous phases contained 0.01 wt.% NaN_3 and their pH were adjusted by dropwise addition of HCl or

NaOH solutions. The mixtures were emulsified using an Ultra-Turrax homogenizer (IKA T25) with a 10 mm mixer head (S25N-10G) operating at 13,500 rpm for 1 min. Emulsions were observed with an Olympus BX51 microscope operating in transmission mode and equipped with an Olympus DP70 camera. The digital images were analyzed using Image-Pro Plus software. The size distributions of the drop populations in the emulsion samples were obtained by measurement of the diameters of at least 50 drops for each sample so that both the surface average diameter $D_{[3,2]}$ and the polydispersity index P defined by equation 2 could be estimated :

$$D_{[3,2]} = \frac{\sum_i N_i D_i^3}{\sum_i N_i D_i^2} ; \quad P = \frac{1}{D_m} \frac{\sum_i N_i D_i^3 |D_m - D_i|}{\sum_i N_i D_i^3} \quad (2)$$

where N_i is the total number of droplets with diameter D_i and D_m is the median diameter, *i.e.* the diameter for which the cumulative undersized volume fraction is equal to 50%.

In order to directly visualize the arrangement of WPM particles at the interface of emulsion drops, cryo-SEM observation of emulsions was carried out with a Quanta 200 scanning electron microscope (FEI, Eindhoven) equipped with liquid nitrogen cooled sample preparation and transfer units. A drop of the sample was placed on the specimen holder before being frozen on a bed of dried ice (-180 °C). The sample was then transferred to the sample preparation unit of the cryo-SEM held at -160 °C and a pressure of 10^{-6} mbar. Once fractured with a blade and coated with a layer of Au-Pd, the sample was inserted into the observation chamber equipped with an SEM cold stage module held at -125 °C. Heptane was preferred to Miglyol 812N as the dispersed phase for these observations, firstly to avoid oil crystallization during the freezing step as heptane solidifying in an amorphous state allows the drops to remain spherical and the interface smooth, and secondly to allow light sublimation of the oil before inserting the sample in the observation chamber. In this case, after fracture of the sample, the preparation chamber temperature was raised to -110 °C for approximately 5 min. before decreasing the temperature again, metalizing and inserting the sample for observation. As will be shown later, both systems (heptane or Miglyol 812N emulsions) display the same overall macroscopic and microscopic behaviour so that the trends observed with cryo-SEM for heptane emulsions can be extrapolated to Miglyol 812N emulsions.

(e) *Determination of the concentration of non-adsorbed WPM particles*

The amount of non-adsorbed WPM particles left in the aqueous phase of emulsions was determined by absorbance measurements using a spectrophotometer (UNICAM UV3) operating at 600 nm where only turbidity induced by microgels contributed to the signal. After emulsification, the emulsions were kept at

rest for 1 hr. in order to allow the drops to form a dense cream at the top of the vessel coexisting with an aqueous subnatant. The subnatant was then removed with a syringe and centrifuged at 5,000 rpm for 5 min. (Eppendorf MiniSpin) in order to remove potential small oil drops still dispersed in the aqueous phase and increasing artificially the overall turbidity. The lower part of the centrifuged subnatant was then used, after re-dispersion of the particles and dilution if needed, for spectrophotometric measurements. The absorbance of dispersions was measured in a 1 cm path length quartz cell (Hellma QS 1000) using background dispersions prepared at the corresponding pH and NaN_3 concentration. The WPM particle concentrations were then estimated by applying the Beer-Lambert law using the extinction coefficient at 600 nm deduced from calibration curves.

RESULTS AND DISCUSSION

We first discuss the behaviour of aqueous dispersions of WPM particles at different pH in the presence and absence of salt. This sets the scene for understanding the properties of o/w emulsions stabilized by such particles. The dependence of the average emulsion drop size on particle concentration is analysed in the framework of the limited coalescence phenomenon, accounting for the presence of non-adsorbed particles, yielding adsorption densities of the particles at the interface. Cryo-SEM is used to observe the arrangement of particles at drop interfaces and confirm the picture emerging from the above. Evidence is given for the formation of bridging particle monolayers as an explanation for the high stability of sparsely covered emulsion drops.

(a) Aqueous dispersions of WPM particles

(i) Effect of sonication

The effect of sonication on a dispersion of the received WPM powder is shown in Figure 1. As already reported by Schmitt *et al.*[31] the WPM particles form during the spray-drying step yielding spherical hollow granules having a diameter of about 30-40 µm. From electron microscopy observations, they showed that the WPM particles constitute the wall of the powder particles where they are densely packed surrounding an empty inner cavity formed by water evaporation during drying. Even if the WPM particles keep their globular shape and do not exhibit any noticeable fusion within the wall of the dried granules, a simple dispersion of the powder particles in water under mild agitation was not sufficient to promote their de-aggregation into individual microgel particles as illustrated by Figure 1(a), where the granule architecture of a freshly prepared powder dispersion can be noticed. After 20 min. of sonication, all the granules have been de-aggregated into a dispersion of individual microgel particles (Figure 1(b)), with typical average

8

hydrodynamic diameter d_h of 235 nm (polydispersity index 0.04) at natural pH of 6.5 (Figure 2). The sonication duration was set in order to ensure total de-aggregation of the granules within the least time; nonetheless it has been checked that the WPM particle hydrodynamic diameter did not evolve significantly with further sonication.
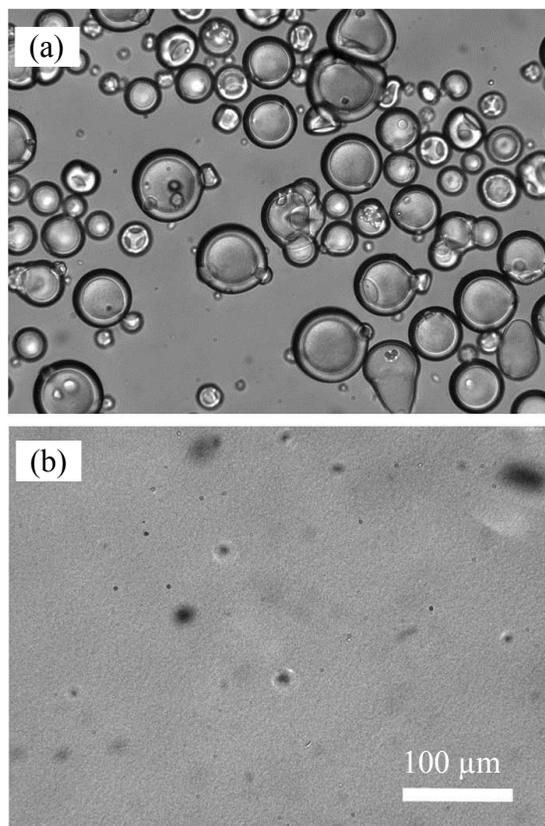
Figure 1. Optical microscopy images of a 4 wt.% WPM aqueous dispersion (a) before and (b) after sonication (scale bar is same in both images).
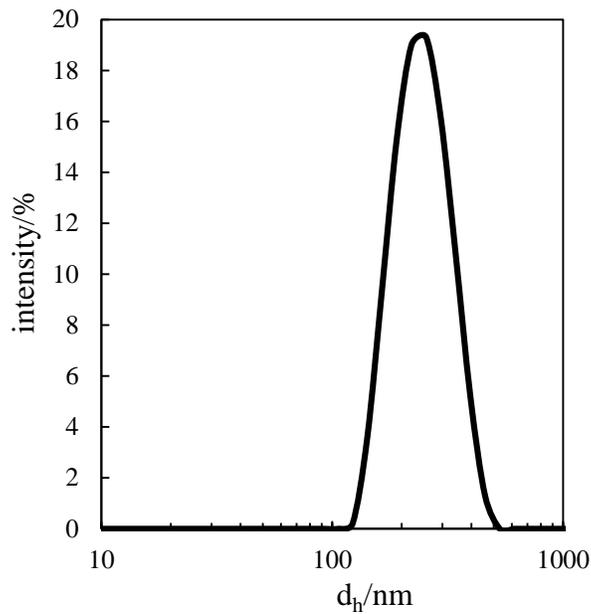
Figure 2. Particle size distribution *via* light scattering of a 0.01 wt.% WPM aqueous dispersion at 25 °C and natural pH (6.5).

(ii) Morphology of WPM particles

In order to assess the impact of the sonication process on the morphology of the particles, comparative TEM observations have been performed on native (after synthesis) and sonicated (after spray-drying) WPM dispersions (4 wt.%). Figure 3 shows two typical micrographs of the dispersions. No significant change in morphology could be detected after sonication, the particles exhibiting in both cases a globular shape. Furthermore, both types of microgel dispersions had similar size distributions, their diameters ranging between 80 and 360 nm, an interval slightly lower compared to the light scattering data which may be due to the dehydration of the particles during sample preparation. Based on this information we conclude that spray-drying and sonication treatments did not alter the physical properties of the WPM.

10
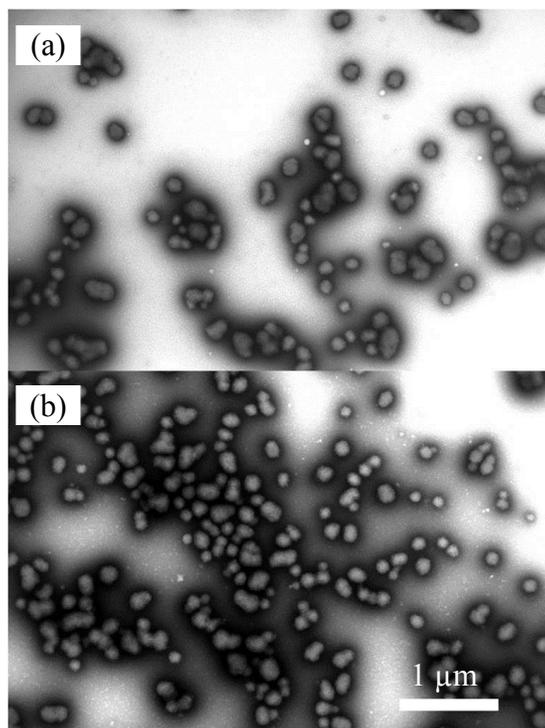
Figure 3. Negative-staining TEM micrographs from 4 wt.% WPM aqueous dispersions; (a) freshly prepared (before spray-draying) and (b) after sonication of spray-dried powder.

(iii) Colloidal stability of aqueous dispersions

We investigated the colloidal stability of 0.1 wt.% WPM dispersions at various pH (adjusted between pH 2 and 8 by dropwise addition of HCl or NaOH solutions) for two different salinities (0 M and 150 mM NaCl). As can be seen in Figure 4(a1) and (b1), three main pH domains can be identified in both cases. In the absence of NaCl, the particles formed stable dispersions at pH below 4.0 or above 5.5. Within the range $4.0 < pH < 5.5$, the dispersions were found to be unstable and quickly sedimented after preparation due to aggregation of the microgel particles as revealed by optical microscopy (Figure 5). The size evolution of the aggregates was found to be related to the aqueous pH value with a minimum around pH 4.8. This behaviour was very well correlated with the variation of the ζ-potential of the particles measured as a function of pH given in Figure 6. The particles display a polyampholyte character with an isoelectric point (IEP) at pH 4.7, where their overall charge is zero, and two pH domains above and below this critical value where the microgel particles are negatively and positively charged respectively. This surface charge evolution is related to the balance between the dissociation of the carboxylic and amino groups of the microgel constitutive whey proteins. The colloidal stability of the dispersions is then mainly triggered by their overall charge, the electrostatic repulsion between particles being high enough to ensure dispersion stability for $pH < 4.0$ or > 5.5 and too low for intermediate pH to counterbalance the attractive interactions that lead to microgel aggregation and ultimately sedimentation. Similar trends were observed in the

11

presence of 150 mM NaCl, see Figure 4(b1). The main difference lies in the observable shift of the instability domain towards acidic pH (3.5 < pH < 5.0) which was confirmed by ζ-potential measurements (Figure 6) showing a decrease of the IEP towards pH 4.2 due to specific protein surface charge screening by Na^+ and Cl^- ions.
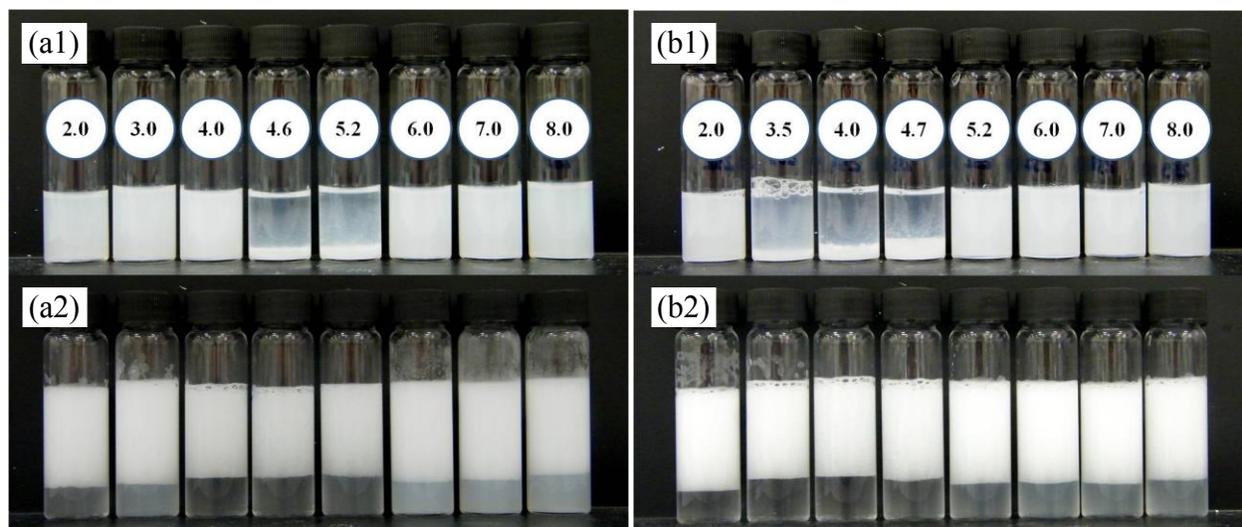
Figure 4. (1) Photographs of vessels containing 0.1 wt.% WPM aqueous dispersions and (2) corresponding o/w emulsions (50 vol.% Miglyol 812N) 1 hr. after preparation as a function of pH (given) and salinity; (a) 0 M NaCl, (b) 150 mM NaCl.
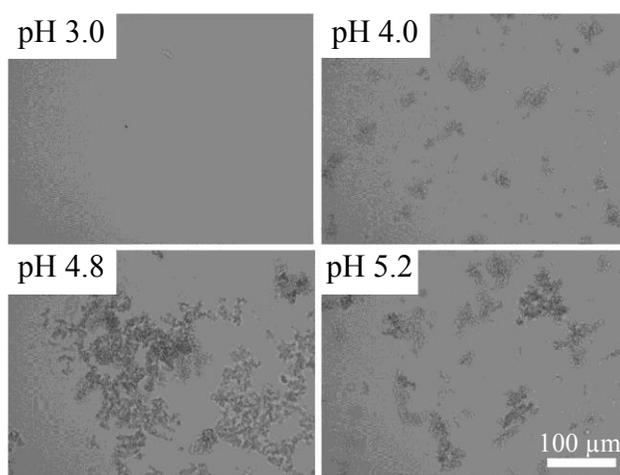
Figure 5. Optical microscopy images of 0.1 wt.% WPM aqueous dispersions without salt 1 hr. after pH adjustment and after gentle manual shaking of the vials.

The pH value of the aqueous phase not only triggered the change in the charge of the microgel particles but also impacted their hydrodynamic diameter as can be seen in Figure 6. Because the microgels are soft

and poorly cross-linked particles swollen by water, their swelling behaviour largely depends on the degree of solvation of the constitutive protein units and on the attractive or repulsive electrostatic interactions between their charges. As a consequence, a minimum of the hydrodynamic diameter was found between pH 4.0 and 5.0 in the absence of salt, corresponding to the domain of charge neutralization (around the IEP), whereas the microgels swell at higher and lower pH where their net charges are higher. An asymmetric swelling behaviour is observed on either side of the IEP, the swelling degree being more pronounced at acidic pH. This feature can be explained by noting that the distribution and degree of ionization of the lateral -COOH and -NH$_2$ groups of the protein amino acids are also asymmetric with respect to the IEP and much more pronounced on the acidic side.[34]
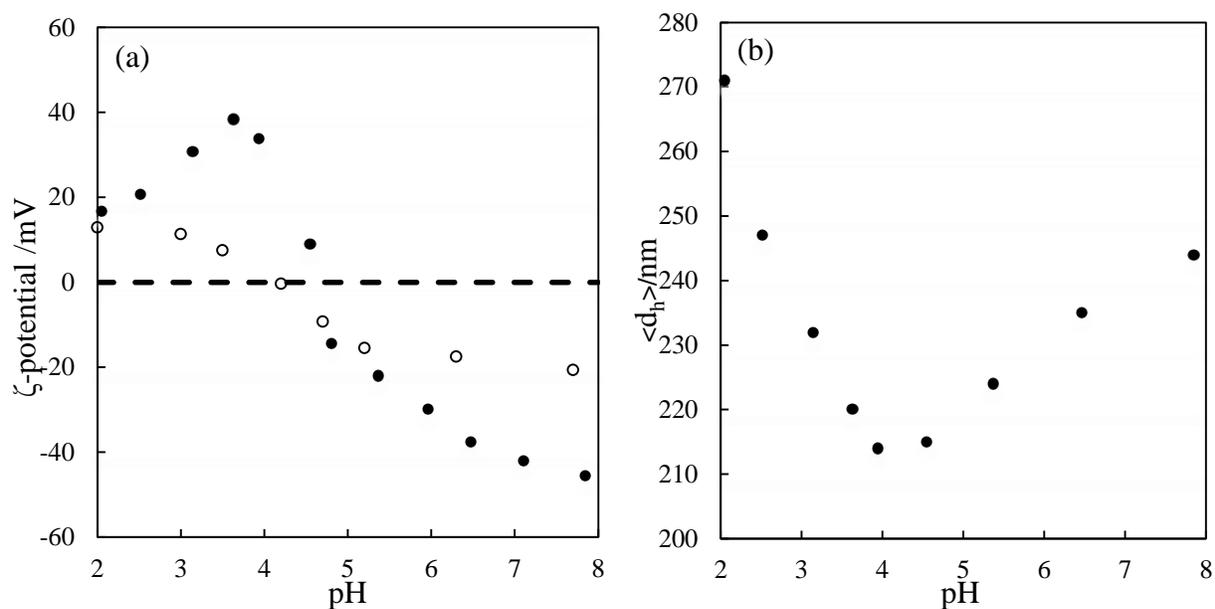
Figure 6. Evolution of (a) ζ-potential and (b) average hydrodynamic diameter of 0.01 wt.% WPM aqueous dispersions at 25 °C as a function of pH and salinity; filled points 0 M, open points 150 mM NaCl. Note the strong reduction of the ζ-potential in the presence of 150 mM due to compression of the electrical double layer at the surface of the WPM.

(b) Oil-in-water emulsions stabilised by WPM particles

(i) Influence of pH and salt concentration

Two series of emulsions were prepared at equal volumes of Miglyol 812N and 0.1 wt.% WPM aqueous dispersion as a function of pH (between 2 and 8) for two salt concentrations (0 and 150 mM NaCl). Photographs of typical samples are shown in Figure 4(a2) and (b2). Over the whole pH range, the produced emulsions were all direct (o/w) and stable to coalescence at rest for at least 18 months. However, because of the size of the drops and the action of buoyancy, the emulsions formed a

13

creamed layer at the top of the vessel within minutes coexisting with a subnatant aqueous phase. Depending on the pH of the aqueous phase, the subnatant was either (i) clear (for 4 < pH < 5.5 without added salt and for pH < 5 with 150 mM NaCl) suggesting complete adsorption of the microgel particles to drop interfaces or (ii) turbid (for the other pH without salt) or slightly turbid (for pH > 5 with 150 mM NaCl) suggesting that a fraction of the particles remained non-adsorbed in the aqueous phase. It is worth noting that the clear subnatants corresponded to the range of pH where the microgel particles were weakly charged (absolute value of ζ-potential < 20 mV) and most often initially aggregated in the aqueous phase.

Optical microscopy observation of the emulsions revealed that the drop characteristics also evolved with pH for the two series. In both cases, three pH domains could be identified. Figure 7 shows microscopy images of typical emulsions in the three pH domains for the two series. Without salt (upper row), emulsions were composed of small, slightly polydisperse (P > 20%) and flocculated drops at low and high pH. The origin of the drop flocculation will be discussed in detail in a later section. At intermediate pH, the emulsions were fluid with discrete and bigger drops exhibiting very narrow size distributions (P < 10%). Although the three pH domains could still be observed, the presence of 150 mM NaCl in the aqueous phase had two main consequences on the emulsion characteristics besides an overall slight increase of the drop sizes (Figure 8). Firstly, the emulsions in the low and high pH ranges were no longer flocculated and drops could flow individually. Secondly, the intermediate pH range was shifted towards more acidic pH (from *ca.* 4 < pH < 5.5 without salt to 3.5 < pH < 5 with salt) as revealed by the study of the drop size evolution with pH shown in Figure 8. Here again the good correlation between the WMP properties in aqueous dispersion and the final emulsion characteristics is worth noting and suggests that the particles adopt different adsorption modes depending on their surface charges.
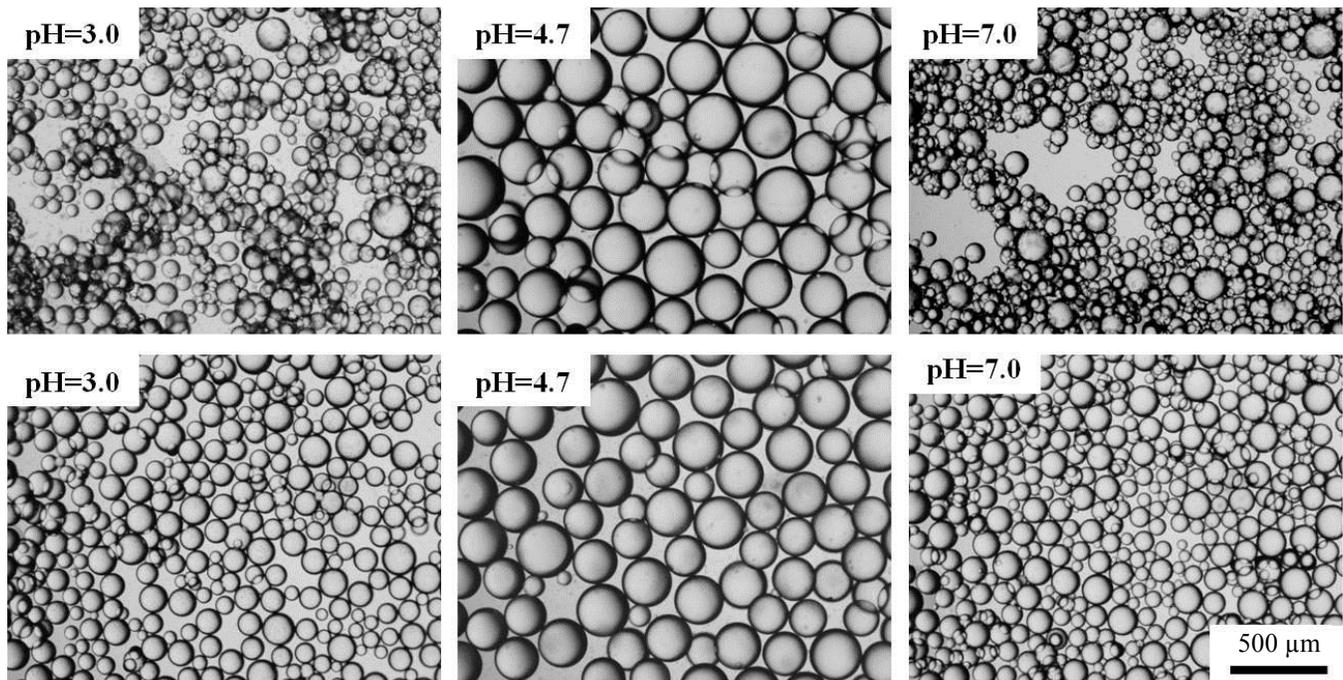
Figure 7. Optical microscopy images of o/w emulsions stabilised by 0.1 wt.% WPM particles as a function of pH and salinity; upper row - 0 M NaCl, lower row - 150 mM NaCl.
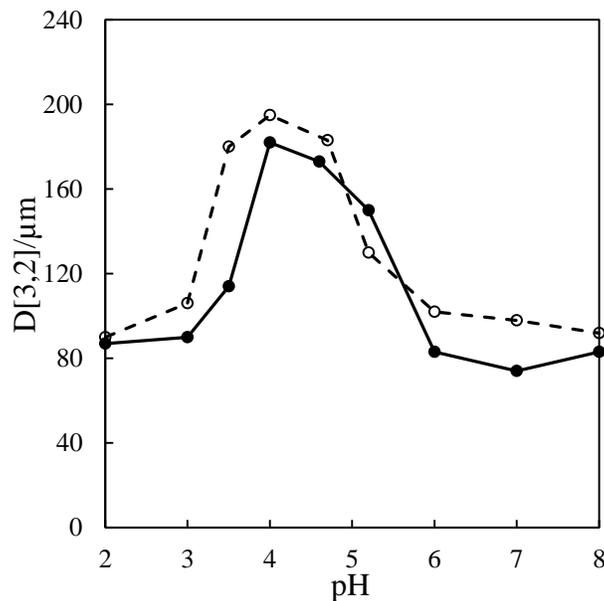
Figure 8. Evolution of the average drop diameter of o/w emulsions stabilised by 0.1 wt.% WPM particles as a function of pH; filled points – 0 M NaCl, open points - 150 mM NaCl.

(ii) Influence of WPM particle concentration

When considering emulsification, two main régimes are generally distinguished depending on the initial emulsifier concentration.[35] In excess of stabiliser (emulsifier-rich régime at high concentration), the final drop size of the emulsion is virtually independent of the initial stabiliser

15

concentration and mainly depends on the stirring intensity which controls drop fragmentation. In contrast, if the system is emulsified at low concentration of stabiliser (emulsifier-poor régime) the newly created drops are initially only partly covered by the emulsifier and experience coalescence events once the agitation is stopped. This coalescence leads to a progressive reduction of the oil-water interfacial area until the stabiliser adsorption density, Γ, becomes high enough to prevent further coalescence events. As a consequence the final drop size is related to the initial stabiliser concentration. In the case of Pickering emulsions, because of the high desorption energy required to remove adsorbed particles, this so-called limited coalescence process has been successfully exploited to prepare stable and nearly monodisperse emulsions (P < 20%) of controlled average drop size[7,8] and used to obtain an insight into particle adsorption and arrangement at the interface[7, 8,36-39]. According to those previous studies, particles adsorb either forming a dense monolayer or a multilayer[7,8,39], but cases where the interfacial coverage was surprisingly low (sub-monolayer) have also been reported[36-38].

For emulsions undergoing limited coalescence, a simple mass balance equation based on geometrical considerations can be written, assuming complete adsorption of spherical particles at the interface[8]:

$$\frac{1}{D_{[3,2]}} = \frac{1-\phi}{6\phi\Gamma}c$$

(3)

where ϕ is the volume fraction of disperse phase, c is the initial emulsifier concentration in water and $D_{[3,2]}$ is the mean drop diameter. This equation predicts that the inverse of the mean drop diameter should vary linearly with c such that Γ can be obtained directly from the slope of $1/D_{[3,2]}$ against c.
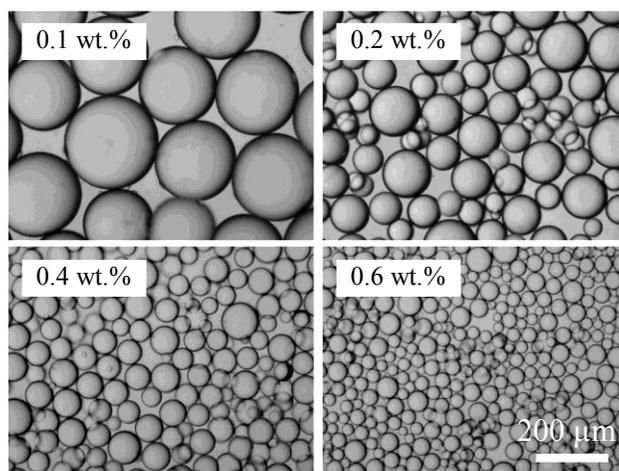
Figure 9. Optical microscopy images of o/w emulsions prepared at pH 4.7 stabilised by WPM particles of different concentration in water immediately after preparation.

For that purpose, a series of emulsions with equal volumes of water and oil phases and different concentrations of WPM particles (0.02-0.6 wt.%) was prepared at three different pH (3.0, 4.7 and 7.0) and two salt concentrations (0 and 150 mM NaCl). In Figure 9 the optical microscopy images show the droplet size evolution as a function of the initial particle concentration for the series at pH 4.7. The more concentrated the initial dispersion, the smaller the drops. This example is representative of the trend observed in all the series. The size distributions of the emulsion drops were determined directly by optical microscopy and the evolution of the inverse drop diameter as a function of particle concentration is plotted in Figure 10. The linear relationship observed initially confirms that such emulsions experience limited coalescence in the emulsifier-poor régime. Within the explored concentration range, one can notice that above a certain particle concentration the linearity is lost for pH 3 and 7 for both salinities which corresponds to the transition towards the emulsifier-rich régime.

From the initial slopes of the plots in Figure 10 and assuming that in these concentration ranges all the emulsifier adsorbs at the drop interfaces, we estimated the WPM interfacial adsorption density, Γ, which are given in Table 1 for the different formulations. For comparison, the adsorption density values of ideal WPM monolayers at the interface, $\Gamma_{90\%}$, are also reported. Those estimations are based on hexagonal close packing of monodisperse, spherical particles with only 90% of the interfacial area being covered. We took from the dynamic light scattering data WPM diameters equal to 235 nm at pH 3.0 and 7.0 and equal to 215 nm at pH 4.7 and a protein density in the water-swollen microgels at pH 3.0 and 7.0 equal to the one at the native pH ($\rho_p = 0.150$ g/cm^3) and equal to 0.196 g/cm^3 at pH 4.7.[40] From this simple approach we could be tempted to conclude that, for both salinities, the interfacial densities correspond closely to those of a monolayer at pH 3.0 and 7.0, and close to 1.5 monolayers at pH 4.7. However, this does not take into account the excess particles that remain dispersed in the aqueous phase at certain pH values (Figure 4).

In order to correct our estimation of Γ to achieve more realistic values, we determined the concentration of non-adsorbed particles left in the subnatant of emulsions by absorbance measurements at 600 nm. The effective interfacial densities calculated from the slopes of the corrected curves are also reported in Table 1 and denoted as $\Gamma_{600\,nm}$. Although this correction did not really impact the values estimated at 150 mM NaCl for the different pH, it had a dramatic influence on the microgel adsorption densities in emulsions without salt, the effective interfacial coverage falling to less than half a monolayer at pH 3.0 and 7.0. As a corollary, the microgel adsorption efficiency, α, can be evaluated as being equal to the ratio $\Gamma_{600\,nm}/\Gamma$. It appears then clearly that most of the microgel particles adsorbed efficiently when neutral ($\alpha > 90\%$) or when their charges were screened by salt addition ($\alpha > 80\%$) whereas only around

half of them actually stabilized the interface when charged in pure water at pH 3 and 7. This limited coalescence study confirmed that the microgel particles exhibited different modes of adsorption as a function of pH and salinity. When neutral, the particles formed aggregates in the aqueous phase. The obtained value of $\Gamma_{600\ nm}$ indicates that it is likely they also adsorbed as small aggregates during emulsification (or re-formed aggregates once at the interface) to achieve drop surface coverages higher than a monolayer. When charged, only a fraction of the particles is actually adsorbed. Furthermore, even if a large number of the microgel particles remain dispersed in the aqueous phase, the emulsifier-poor régime was still observed as demonstrated by the linear dependency of the inverse drop diameter as a function of the initial WPM concentration. To the authors knowledge this is the first time that the limited
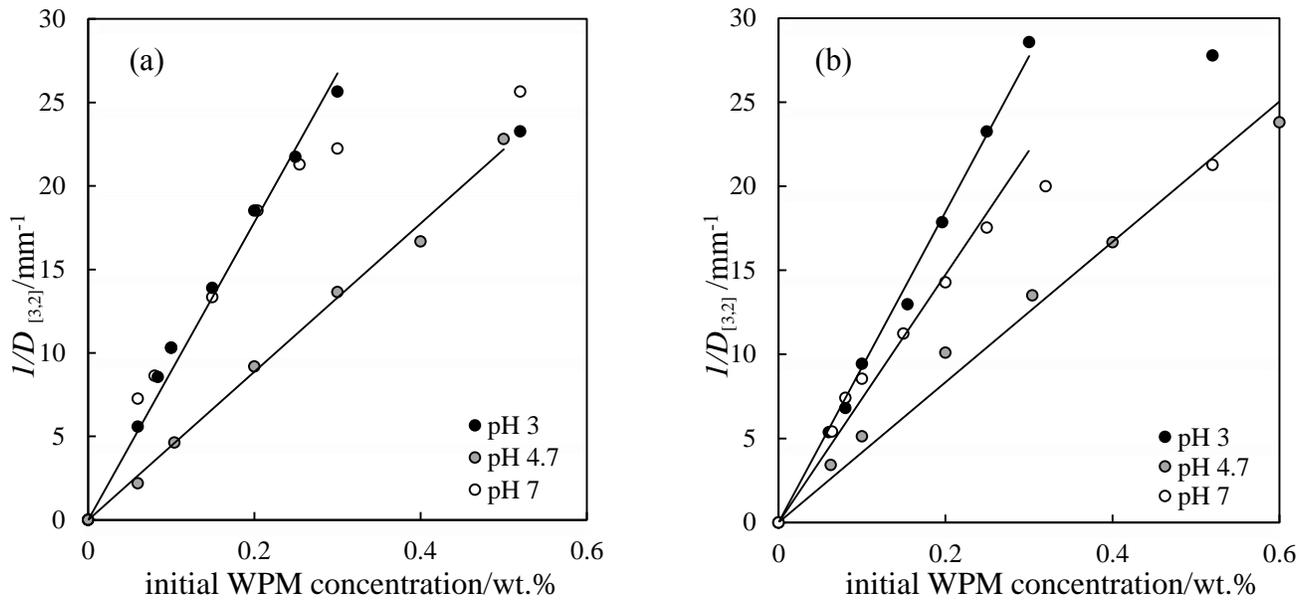
Figure 10. Evolution of the inverse of the average drop diameter ($1/D_{[3,2]}$) for Miglyol 812N-in-water emulsions as a function of the initial WPM particle concentration, c, in the aqueous phase for three different pH; (a) 0 M NaCl, (b) 150 mM NaCl.

	0 M NaCl			150 mM NaCl		
	pH 3.0	**pH 4.7**	**pH 7.0**	**pH 3.0**	**pH 4.7**	**pH 7.0**
Γ/mg m^{-2}	18.3	37.9	18.7	18.1	40.7	22.8
$\Gamma_{90\%}$/mg m^{-2}	21.2	25.3	21.2	21.2	25.3	21.2
$\Gamma_{600\ nm}$/mg m^{-2}	9.5	36.1	8.6	18.1	36.7	18.5
α/%	51.9	95.2	46.0	100.0	90.2	81.1

Table 1. Interfacial adsorption densities and adsorption ratio within the emulsifier-poor régime for Miglyol 812N-in-water emulsions stabilised by WPM particles at different pH and salinities. Γ is the adsorption density deduced from the limited coalescence model assuming all particles adsorb, $\Gamma_{90\%}$ is the density corresponding to the adsorption of an ideal monolayer of close-packed monodisperse spherical

18

particles, $\Gamma_{600\,nm}$ is the corrected effective adsorption density after accounting for non-adsorbed particles and α is the adsorption efficiency of the particles (= $\Gamma_{600\,nm}/\Gamma$).

coalescence phenomenon is reported for emulsions exhibiting an excess of particles. This linear relationship then implies adsorption of a constant fraction of particles, equal to α, independent of the initial concentration. This indicates that one cannot consider the microgel particles as strictly identical but that subtle differences in their characteristics (size, surface charge, protein composition, degree of crosslinking *etc*.) might be important enough to induce differences in their adsorption behaviour. One of the most obvious parameters that could be responsible for this behavior is the surface charge density of the particles. Two different mechanisms may occur. An increased charge density results in an increased hydrophilicity (*i.e.* a decreasing θ) and we can suppose that some of the particles became too hydrophilic to adsorb at the given pH and remain dispersed in water. Another aspect to consider when dealing with charged particles is the electrostatic barrier they have to overcome to adsorb at a charged oil-water interface, which may be the case at certain pH. The probability of particle adsorption will then be related to the balance between the repulsive electrostatic force and the hydrodynamic force that pushes the particle towards the interface during emulsification. Because these forces are dependent not only on the charges but also on the particle size, this latter parameter may become decisive in determining particle attachment in the specific case of the two forces being of the same order of magnitude.[35] Finally, addition of 150 mM NaCl to the aqueous phase did not affect the colloidal stability of the WPM dispersions at pH 3 and 7 (stable dispersion of well dispersed particles) but changed drastically their adsorption efficiency since almost all the particles were associated with the emulsions ($\alpha > 80\%$). The high electrolyte concentration enhances the hydrophobicity of the particles (increasing θ) and/or suppresses the electrostatic barrier limiting the adsorption by screening the charges. The majority of the particles can then be anchored at the interface and arranged as a quasi-compact monolayer.

(iii) Cryo-SEM observations of the emulsion droplet interface

From the estimates of $\Gamma_{600\,nm}$, one supposes that drop recombination was stopped during the final stage of limited coalescence by steric repulsion between adsorbed particles on separate drops due to the formation of a quasi-monolayer (in the presence of salt) or a multilayer (when neutral). However it is surprising to see that drop coalescence halted at an early stage when the particles were charged at low salt concentration. This resulted in stable emulsions with interfacial adsorption densities corresponding to less than half an ideal monolayer. Particle assembly appears then as a critical issue to understand the stability of such emulsions. Cases of stable emulsions exhibiting low interfacial coverage have already been

reported in the literature with the particles either forming well ordered long-range colloidal crystals or 2-D clusters resulting in non-homogeneous coverage.[37,38,41] In the specific case of soft microgel particles, recent papers also report the interesting ability of particles to deform and spread at the interface covering a much larger surface area than their initial hydrodynamic diameter would suggest and as a consequence leading to lower adsorption densities than expected.[36,42] In order to characterize the WPM organisation at droplet interfaces, we performed cryo-SEM measurements on heptane-in-water emulsions stabilised by the same particles. Before doing so however we first checked that systems containing this oil did not change either the emulsion characteristics or the particle adsorption behavior as a function of pH; that this is so is illustrated in Figures S1 and S2.

An example cryo-SEM image of one heptane drop covered by microgel particles at pH 3 is shown in Figure 11. During sample fracture the frozen oil constituting the drop has been removed forming a cavity and allowing direct visualisation from above of particles residing at the interface. The particle organisation at different pH is illustrated in Figure 12 where closer views of the interface are shown. At pH 4.8, the interface was covered by a continuous 2-D network of highly aggregated particles whereas at extremes of pH particles adopted discrete configurations of either individual particles/small aggregates (pH 3) or larger aggregates forming 2-D flocs surrounded by what appears to be bare interface (pH 7). Those configurations obviously need interpreting with caution since clear observations of the interface were difficult to obtain and because of the possible artifacts induced by the technique. Nonetheless these observations were *a priori* consistent with our estimation of the corrected interfacial adsorption density values, $\Gamma_{600\ nm}$ (Table 1). In order to further characterise the interfacial structure, we performed light partial sublimation of the samples to remove the residual heptane layer remaining at the interface and to promote light dehydration of the particles. As shown in Figure 13, this process revealed the presence of surface-active material forming a thin membrane at the interface between the particle aggregates suggesting that the initial cryo-SEM observations (Figures 11 and 12) without sublimation did not allow us to fully visualise the entire surface. This interstitial material may have different origins: it may be due to (i) impurities associated with the synthesis of WPM or released during their dispersion by sonication (*e.g.* as proteose peptone residues), (ii) the de-aggregation into subunits of some WPM at the interface during emulsification or (iii) the spreading of the microgel particles at the interface as was reported for other soft particles used as emulsifiers.[36] Particle de-aggregation seems unlikely since no alteration of the microgel structure could be detected after sonication but their spreading at the interface could result in the formation of a very thin and continuous layer of flattened and inter-penetrated particles within which individual particles are hardly noticeable. These two latter hypotheses were supported by the film relief, revealed by sublimation in Figure 13, which was formed of almost regularly spaced bumps,

either reminiscent of initial particles before deformation or denoting the presence of smaller protein aggregates (microgel subunits) at the interface but which didn't allow us to discriminate between the two potential causes.
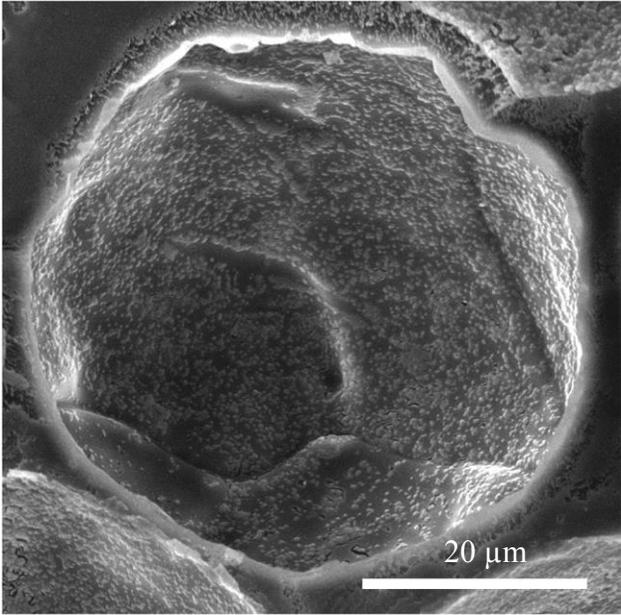
Figure 11. Cryo-SEM image of a heptane emulsion drop in water (no salt) covered by 0.1 wt.% WPM particles at pH 3. During fracturing, the frozen oil has been removed allowing direct visualisation of the particles residing at the interface.
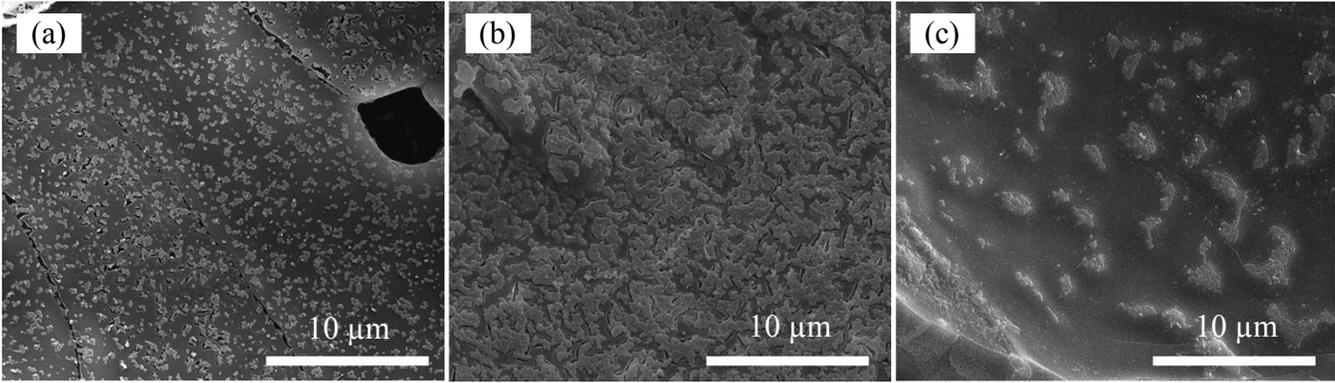
Figure 12. Cryo-SEM images of the interface of heptane-in-water (no salt) emulsions stabilised by 0.1 wt.% WPM particles: (a) pH 3 - discrete organisation of individual particles or small aggregates, (b) pH 4.8 – 2-D gel of aggregated particles and (c) pH 7 - flocs of particles.
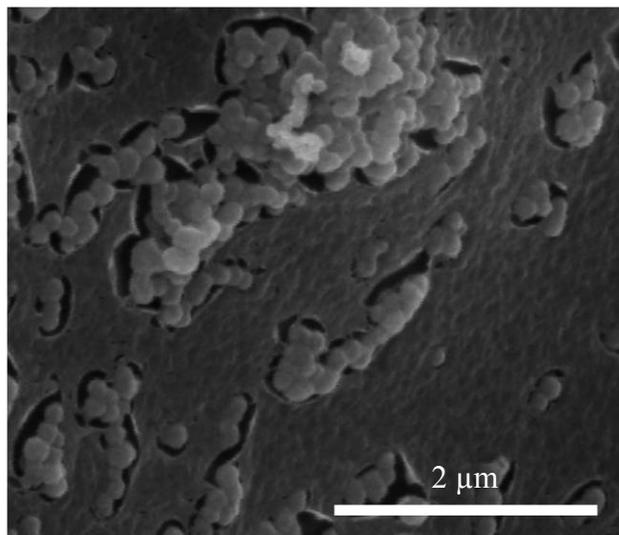
Figure 13. Cryo-SEM image of the interface of a heptane-in-water emulsion stabilised by WPM particles at pH 4.8 after light sublimation. The sublimation reveals the presence of a thin film between the particle aggregates.

(iv) Origin of the stability of poorly covered emulsion drops and their flocculation

As mentioned previously, o/w emulsions stabilized by WPM particles were flocculated at low electrolyte concentrations and at pH where the particles were significantly charged ($\alpha \approx 50\%$). In these conditions, the flocculated drops were in close contact and experienced attraction that was responsible for the formation of flat adhesive films between them which appeared as white ellipses in optical microscopy as shown Figure 14(a). The stability and the structure of these thin films are thus critical in determining the resistance of adjacent drops toward coalescence and in determining the overall lifetime of emulsions. Considering particle-stabilized emulsions, two types of limiting configuration can be imagined for the adhesive film structure: the particles may form either a bilayer or a monolayer that prevents the film from draining and breaking. In the case of a monolayer, the particles form a dense patch bridging the two interfaces of the adjacent drops. Several examples of such a configuration have already been reported in the literature, either with isolated emulsion films where two colloid-laden interfaces are brought into contact in a controlled manner[43-45] or with emulsions[41,46-48]. In particular, bridging monolayer formation has been strongly hypothesised and demonstrated for emulsions containing drops sparsely protected by charged particles (with a surface coverage as low as 5%) and seems to be at the origin of the astonishing kinetic stability of the emulsions due to spontaneous particle accumulation in the contact zone between drops forming a locally dense particle layer that provides steric hindrance against drop coalescence.[37,38,43,49] Bridging not only occurs with rigid particles but also with soft particles that are able to deform and span two interfaces as reported recently in a study on temperature-sensitive poly(NIPAM)-based microgels.[48] In this latter case the flocculation extent due to bridging has

been found to be related to the degree of deformability of the particles and to be highly dependent on the emulsion preparation pathway (temperature and energy of emulsification).[42,48]

In order to understand the origin of the emulsion stability and flocculation and to resolve the structure of the adhesive films, we performed direct cryo-SEM visualisation of contact zones between drops. It revealed the spontaneous concentration of WPM particles forming dense discoid layers bridging the neighbouring drops, as can be seen in Figure 14(b), whereas the rest of the drop interface remained poorly covered by particles. Such preferential location of the particles is then at the origin of the stability of the emulsions despite the very low surface coverage of drops. The drop adhesion is due to the bridging of the interfaces by the particles. The formation of such adhesive films is a dynamic process. In order to bridge, particles on one interface have to access free areas on the opposing interface. During film thinning, water drainage tends to drag particles away from the contact area. The interfacial mobility of the particles is then important; the small aggregates covering the interface at pH 3 and 7 will then be more easily squeezed away liberating free interface to be bridged compared with the 2-D gel formed when the particles are neutral or the denser layer formed at pH 3 and 7 when salt is added providing good steric and mechanical stabilisation against bridging.
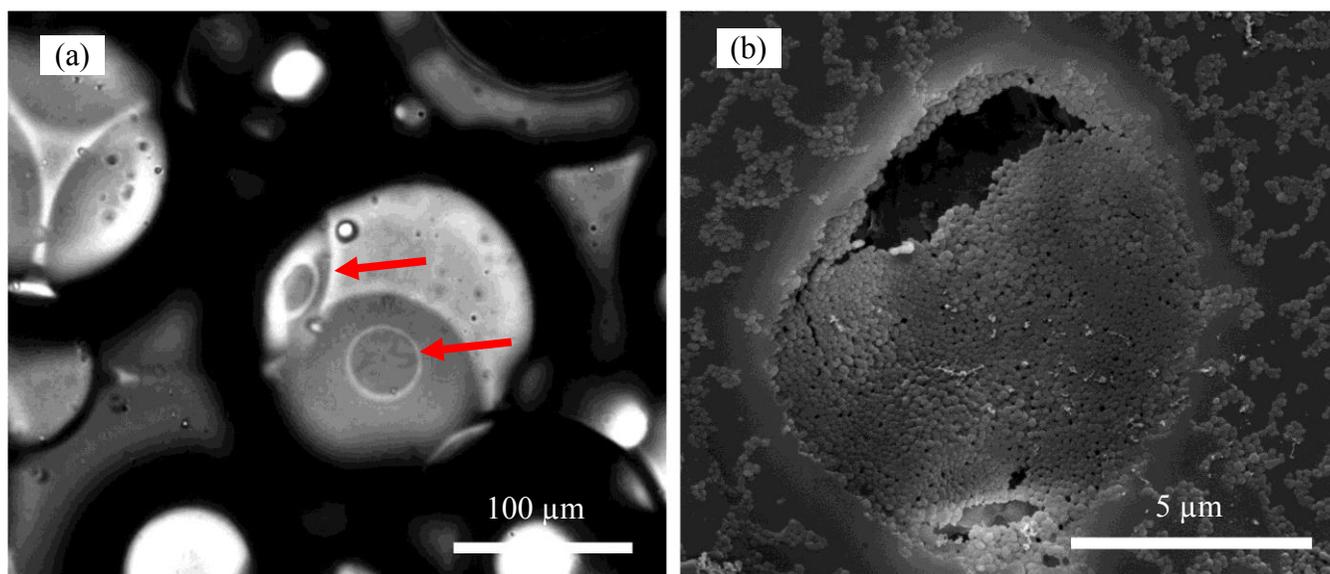
Figure 14. (a) Optical microscopy image of flat adhesive films (indicated by red arrows) between flocculated heptane drops in an o/w emulsion stabilised by WPM at pH 6 and (b) cryo-SEM image of a flat adhesive film between two heptane drops in water at pH 6 viewed from above. The contact zone between the drops forms a disc of close packed particles; note the lower concentration of adsorbed particles outside of this zone.

(v) Role of impurities on emulsion stability

In order to shed light on the influence of small molecule impurities on the emulsion characteristics, we performed additional experiments by filtering WPM dispersions. A 0.1 wt.% WPM dispersion was filtered through a 100 nm pore membrane (Acrodisc syringe filter), the filtered solution being collected to perform oil-water interfacial tension measurements. Figure 15(a) shows the comparative evolution of the Miglyol 812N-water tension with time for the initial WPM dispersion and the filtrate (deprived of particles) at pH 7. As can be seen, the equilibrium tension decreased from 20.5 mN m^{-1} using pure water to 11.3 mN m^{-1} for the raw dispersion and to only slightly higher at 12.5 mN m^{-1} for the filtrate. This simple experiment confirmed the presence of small surface-active impurities within the WPM dispersions and showed that most of the interfacial tension decrease could be attributed to them. Nonetheless despite this, an emulsion prepared with only the filtrate was highly unstable to coalescence separating within a few days as shown in the inset of Figure 15(a). Without excluding a potential influence of the impurities on particle-stabilised emulsion properties, this experiment demonstrates that impurities alone cannot be at the origin of the excellent emulsion stability. Furthermore emulsions stabilised with raw WPM dispersions exhibited outstanding stability and resistance towards coalescence as illustrated by Figure 15(b) where an emulsion with millimeter-sized drops is shown to be stable even 8 months after preparation. Such emulsions cannot be obtained with low molecular weight surface-active species alone.
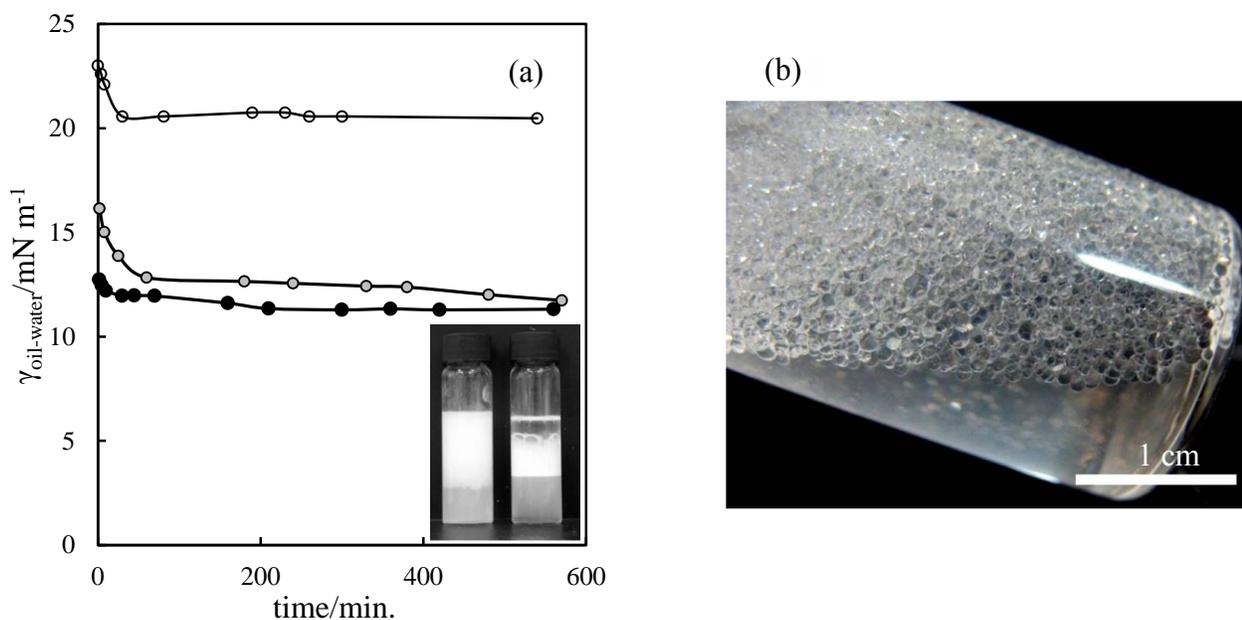
Figure 15. (a) Evolution of the Miglyol 812N-water interfacial tension at 25 ºC with time for 3 different aqueous phases at pH 7: open circles - pure water, filled circles - 0.1 wt.% WPM, grey circles - filtrate of 0.1 wt.% WPM dispersion. Insert – photo' of emulsions 2 days after preparation stabilised by (left) 0.1 wt.% WPM and (right) the filtrate obtained after filtration of 0.1 wt.% WPM dispersion through a 100 nm pore membrane. (b) Photograph of vessel containing Miglyol 812N-in-water (1:1) emulsion with millimetre-sized drops stabilised by 0.025 wt.% WPM at pH 7 with 150 mM NaCl eight months after preparation by hand shaking and stored at room temperature.

CONCLUSIONS

We have investigated the ability of a new class of food-grade particles to act as efficient emulsion stabilizers. The sub-micron whey protein microgels stabilized triglyceride oil-in-water emulsions over the whole range of pH and salinity explored. All emulsions exhibited long term stability with exceptional resistance to coalescence as demonstrated by the production of emulsions with millimeter-sized drops. Clear correlations exist between the microgel properties in aqueous dispersion and the final emulsion characteristics. For conditions where the microgel particles were neutral, they stabilized fluid emulsions with relatively large drops exhibiting narrow size distributions, whereas when they were charged the resulting emulsions were constituted of small, slightly poydisperse and flocculated drops. By coupling optical microscopy observations and spectrophotometry measurements, we characterized the interfacial adsorption densities of the particles using limited coalescence analysis and showed that the adsorption efficiency strongly depends on the particle charge or the salinity of the aqueous phase. Two adsorption modes were found. Almost total adsorption of the particles was obtained when they were neutral or when their charges were screened by salt addition resulting in at least one monolayer at the interface. By contrast, only 50% of the particles adsorbed when they were charged and the resulting emulsion drops were covered by less than half a monolayer. Those estimations were supported by direct visualization of drop interfaces by cryo-SEM. Near the IEP the particles were highly aggregated and formed a continuous 2-D network at the interface; otherwise they organized as individual aggregates separated by particle-free regions. Partial sublimation of the samples suggested that some particles spread at the interface leading to the formation of a continuous protein membrane, where the particles were no longer individually distinguished, that covered the large interface area between the aggregates. Charged particles displayed the ability to bridge opposing interfaces of neighbouring drops to form dense particle disks protecting drops against coalescence and being at the origin of the flocculation and stability of the emulsions containing poorly covered drops. Whey protein microgels are thus a promising new type of food-grade particle for preparing dispersed liquid materials with original properties of interest to the food industry.

REFERENCES

1.   Pickering, S.U., Emulsions. *J. Chem. Soc.* **1907,** 91, 2001-2021.

2.   Ramsden, W., Separation of solids in the surface-layers of solutions and "suspensions" - preliminary account. *Proc. R. Soc.* **1903,** 72, 156-164.

3.   Binks, B.P., Particles as surfactants--similarities and differences. *Curr. Opin. Colloid & Interface Sci.* **2002,** 7, 21-41.

4.   Leal-Calderon, F.; Schmitt, V., Solid-stabilized emulsions. *Curr. Opin. Colloid & Interface Sci.* **2008,** 13, 217-227.

5.   Bancroft, W.D., The theory of emulsification, V. *J. Phys. Chem.* **1913,** 17, 501-519.

6.   Finkle, P.; Draper, H.D.; Hildebrand, J.H., The Theory of Emulsification. *J. Am. Chem. Soc.* **1923,** 45, 2780-2788.

7.   Arditty, S.; Schmitt, V.; Giermanska-Kahn, J.; Leal-Calderon, F., Materials based on solid-stabilized emulsions. *J. Colloid Interface Sci.* **2004,** 275, 659-664.

8.   Arditty, S.; Whitby, C.P.; Binks, B.P.; Schmitt, V.; Leal-Calderon, F., Some general features of limited coalescence in solid-stabilized emulsions. *Eur. Phys. J. E* **2003,** 11, 273-281.

9.   Aveyard, R.; Binks, B.P.; Clint, J.H., Emulsions stabilised solely by colloidal particles. *Adv. Colloid Interface Sci.* **2003,** 100–102, 503-546.

10.   Aussillous, P.; Quéré, D., Liquid marbles. *Nature* **2001,** 411, 924-927.

11.   Binks, B.P.; Boa, A.N.; Kibble, M.A.; MacKenzie, G.; Rocher, A., Sporopollenin capsules at fluid interfaces: Particle-stabilised emulsions and liquid marbles. *Soft Matter* **2011,** 7, 4017-4024.

12.   Adelmann, H.; Binks, B.P.; Mezzenga, R., Oil powders and gels from particle-stabilized emulsions. *Langmuir* **2012,** 28, 1694-1697.

13.   Binks, B.P.; Murakami, R., Phase inversion of particle-stabilized materials from foams to dry water. *Nature Mater.* **2006,** 5, 865-869.

14.   Murakami, R.; Moriyama, H.; Yamamoto, M.; Binks, B.P.; Rocher, A., Particle stabilization of oil-in-water-in-air materials: Powdered emulsions. *Adv. Mater.* **2012,** 24, 767-771.

15.   Stocco, A.; Rio, E.; Binks, B.P.; Langevin, D., Aqueous foams stabilized solely by particles. *Soft Matter* **2011,** 7, 1260-1267.

16.   Gonzenbach, U.T.; Studart, A.R.; Tervoort, E.; Gauckler, L.J., Ultrastable Particle-Stabilized Foams. *Angew. Chemie Int. Ed.* **2006,** 45, 3526-3530.

17.   Dickinson, E., Food emulsions and foams: Stabilization by particles. *Curr. Opin. Colloid & Interface Sci.* **2010,** 15, 40-49.

18.   Dickinson, E., Use of nanoparticles and microparticles in the formation and stabilization of food emulsions. *Trends in Food Sci. & Technol.* **2012,** 24, 4-12.

19.   Wege, H.A.; Kim, S.; Paunov, V.N.; Zhong, Q.; Velev, O.D., Long-term stabilization of foams and emulsions with in-situ formed microparticles from hydrophobic cellulose. *Langmuir* **2008,** 24, 9245-9253.

20.   Kalashnikova, I.; Bizot, H.; Cathala, B.; Capron, I., New pickering emulsions stabilized by bacterial cellulose nanocrystals. *Langmuir* **2011,** 27, 7471-7479.

21.   Tzoumaki, M.V.; Moschakis, T.; Kiosseoglou, V.; Biliaderis, C.G., Oil-in-water emulsions stabilized by chitin nanocrystal particles. *Food Hydrocoll.* **2011,** 25, 1521-1529.

22.   Paunov, V.N.; Cayre, O.J.; Noble, P.F.; Stoyanov, S.D.; Velikov, K.P.; Golding, M., Emulsions stabilised by food colloid particles: Role of particle adsorption and wettability at the liquid interface. *J. Colloid Interface Sci.* **2007,** 312, 381-389.

23.   Liu, F.; Tang, C.H., Soy protein nanoparticle aggregates as pickering stabilizers for oil-in-water emulsions. *J. Agric. Food Chem.* **2013,** 61, 8888-8898.

24.   Murray, B.S.; Durga, K.; Yusoff, A.; Stoyanov, S.D., Stabilization of foams and emulsions by mixtures of surface active food-grade particles and proteins. *Food Hydrocoll.* **2011,** 25, 627-638.

25.   Yusoff, A.; Murray, B.S., Modified starch granules as particle-stabilizers of oil-in-water emulsions. *Food Hydrocoll.* **2011,** 25, 42-55.

26.   Tan, Y.; Xu, K.; Niu, C.; Liu, C.; Li, Y.; Wang, P.; Binks, B.P., Triglyceride–water emulsions stabilised by starch-based nanoparticles. *Food Hydrocoll.* **2014,** 36, 70-75.

27.   Luo, Z.; Murray, B.S.; Yusoff, A.; Morgan, M.R.A.; Povey, M.J.W.; Day, A.J., Particle-stabilizing effects of flavonoids at the oil-water interface. *J. Agric. Food Chem.* **2011,** 59, 2636-2645.

28.   Gupta, R.; Rousseau, D., Surface-active solid lipid nanoparticles as Pickering stabilizers for oil-in-water emulsions. *Food and Function* **2012,** 3, 302-311.

29.   de Folter, J.W.J.; van Ruijven, M.W.M.; Velikov, K.P., Oil-in-water Pickering emulsions stabilized by colloidal particles from the water-insoluble protein zein. *Soft Matter* **2012,** 8, 6807-6815.

30.   Nicolai, T.; Britten, M.; Schmitt, C., β-Lactoglobulin and WPI aggregates: Formation, structure and applications. *Food Hydrocoll.* **2011,** 25, 1945-1962.

31.   Schmitt, C.; Moitzi, C.; Bovay, C.; Rouvet, M.; Bovetto, L.; Donato, L.; Leser, M.E.; Schurtenberger, P.; Stradner, A., Internal structure and colloidal behaviour of covalent whey protein microgels obtained by heat treatment. *Soft Matter* **2010,** 6, 4876-4884.

32.   O'Brien, R.W., Electro-acoustic effects in a dilute suspension of spherical particles. *J. Fluid Mech.* **1988,** 190, 71-86.

33.   Zuidema, H.H.; Waters, G.W., Ring Method for Determination of Interfacial Tension. *Ind. Eng. Chem.***1941,** 13, 312-313.

34.   Fogolari, F.; Ragona, L.; Licciardi, S.; Romagnoli, S.; Michelutti, R.; Ugolini, R.; Molinari, H., Electrostatic properties of bovine β-Lactoglobulin. *Proteins: Structure, Function and Genetics* **2000,** 39, 317-330.

35.   Tcholakova, S.; Denkov, N.D.; Lips, A., Comparison of solid particles, globular proteins and surfactants as emulsifiers. *Phys. Chem. Chem. Phys.* **2008,** 10, 1608-1627.

36.   Destribats, M.; Lapeyre, V.; Wolfs, M.; Sellier, E.; Leal-Calderon, F.; Ravaine, V.; Schmitt, V., Soft microgels as Pickering emulsion stabilisers: Role of particle deformability. *Soft Matter* **2011,** 7, 7689-7698.

37.   Destribats, M.; Ravaine, S.; Heroguez, V.; Leal-Calderon, F.; Schmitt, V., Outstanding stability of poorly-protected pickering emulsions. *Progr. Colloid and Polymer Sci.* **2010,** 137, 13-18.

38.   Gautier, F.; Destribats, M.; Perrier-Cornet, R.; Dechézelles, J-F.; Giermanska, J.; Héroguez, V.; Ravaine, S.; Leal-Calderon, F.; Schmitt, V., Pickering emulsions with stimulable particles: From highly- to weakly-covered interfaces. *Phys. Chem. Chem. Phys.* **2007,** 9, 6455-6462.

39.   Destribats, M.; Lapeyre, V.; Sellier, E.; Leal-Calderon, F.; Schmitt, V.; Ravaine, V., Water-in-Oil Emulsions Stabilized by Water-Dispersible Poly(N-isopropylacrylamide) Microgels: Understanding Anti-Finkle Behavior. *Langmuir* **2011,** 27, 14096-14107.

40.   Phan-Xuan, T.; Durand, D.; Nicolai, T.; Donato, L.; Schmitt, C.; Bovetto, L., On the Crucial Importance of the pH for the Formation and Self-Stabilization of Protein Microgels and Strands. *Langmuir* **2011,** 27, 15092-15101.

41.   Horozov, T.S.; Binks, B.P., Particle-stabilized emulsions: A bilayer or a bridging monolayer? *Angew. Chemie Int. Ed.* **2006,** 45, 773-776.

42.   Destribats, M.; Wolfs, M.; Pinaud, F.; Lapeyre, V.; Sellier, E.; Schmitt, V.; Ravaine, V., Pickering Emulsions Stabilized by Soft Microgels: Influence of the Emulsification Process on Particle Interfacial Organization and Emulsion Properties. *Langmuir* **2013,** 29, 12367-12374.

43.   Horozov, T.S.; Aveyard, R.; Clint, J.H.; Neumann, B., Particle Zips: Vertical Emulsion Films with Particle Monolayers at Their Surfaces. *Langmuir* **2005,** 21, 2330-2341.

44.   Stancik, E.J.; Fuller, G.G., Connect the drops: Using solids as adhesives for liquids. *Langmuir* **2004,** 20, 4805-4808.

45.   Stancik, E.J.; Kouhkan, M.; Fuller, G.G., Coalescence of Particle-Laden Fluid Interfaces. *Langmuir* **2004,** 20, 90-94.

46.   Frost, D.S.; Schoepf, J.J.; Nofen, E.M.; Dai, L.L., Understanding droplet bridging in ionic liquid-based Pickering emulsions. *J. Colloid Interface Sci.* **2012,** 383, 103-109.

47.   Lee, M.N.; Chan, H.K.; Mohraz, A., Characteristics of Pickering Emulsion Gels Formed by Droplet Bridging. *Langmuir* **2011,** 28, 3085-3091.

48.   Destribats, M.; Lapeyre, V.; Sellier, E.; Leal-Calderon, F.; Ravaine, V.; Schmitt, V., Origin and Control of Adhesion between Emulsion Drops Stabilized by Thermally Sensitive Soft Colloidal Particles. *Langmuir* **2012,** 28, 3744-3755.

49.   Vignati, E.; Piazza, R.; Lockhart, T.P., Pickering emulsions: Interfacial tension, colloidal layer morphology, and trapped-particle motion. *Langmuir* **2003,** 19, 6650-6656.